International Scholarly Research Network
ISRN Spectroscopy
Volume 2012, Article ID 256326, 11 pages
doi:10.5402/2012/256326

Research Article

Fluorescence Rejection by Shifted Excitation Raman Difference Spectroscopy at Multiple Wavelengths for the Investigation of Biological Samples

Kay Sowoidnich and Heinz-Detlef Kronfeldt

Institut für Optik und Atomare Physik, Technische Universität Berlin, Sekretariat EW 0-1, Hardenbergstraße 36, 10623 Berlin, Germany

Correspondence should be addressed to Kay Sowoidnich, kay.sowoidnich@mailbox.tu-berlin.de

Received 26 May 2012; Accepted 12 June 2012

Academic Editors: M. Ivanda, S. Magazù, and P. Ribeiro-Claro

Shifted excitation Raman difference spectroscopy (SERDS) was applied for an effective fluorescence removal in the Raman spectra of meat, fat, connective tissue, and bone from pork and beef. As excitation light sources, microsystem diode lasers emitting at 783 nm, 671 nm, and 488 nm each incorporating two slightly shifted excitation wavelengths with a spectral difference of about 10 cm^{-1} necessary for SERDS operation were used. The moderate fluorescence interference for 783 nm excitation as well as the increased background level at 671 nm was efficiently rejected using SERDS resulting in a straight horizontal baseline. This allows for identification of all characteristic Raman signals including weak bands which are clearly visible and overlapping signals that are resolved in the SERDS spectra. At 488 nm excitation, the spectra contain an overwhelming fluorescence interference masking nearly all Raman signals of the probed tissue samples. However, the essentially background-free SERDS spectra enable determining the majority of characteristic Raman bands of the samples under investigation. Furthermore, 488 nm excitation reveals prominent carotenoid signals enhanced due to resonance Raman scattering which are present in the beef samples but absent in pork tissue enabling a rapid meat species differentiation.

1. Introduction

Due to its fingerprinting characteristics, Raman spectroscopy is well suited for the investigation of biological material, for example, for rapid and nondestructive identification purposes. Here, excitation wavelengths in the visible or near-infrared range are preferable to avoid strong absorption of water leading to sample heating [1]. For that reason, in situ Raman investigations are possible since no sample pretreatments, as for example, drying procedures, are necessary. According to the λ^{-4}-dependence of the Raman scattering intensity, the application of shorter excitation wavelengths can significantly improve the spectral quality. On the other hand, this leads to an increased fluorescence interference partly or completely obscuring the Raman signals and thus making the detection of useful spectra hardly possible.

There exist certain methods to remove the fluorescence background from the Raman spectra to overcome the fluorescence issue. In that way, mathematical approaches as polynomial [2] or advanced subtraction methods [3] as well as experimental techniques using a temporal discrimination of the slower fluorescence emission against the Raman photons [4, 5] were successfully applied. As a technique additionally removing the fixed-pattern noise arising from CCD detectors, shifted excitation Raman difference spectroscopy (SERDS) [6] offers a promising alternative. SERDS application requires excitation laser sources with two narrow emission lines spectrally separated in the order of the full width at half maximum of the Raman signals under investigation [7]. In that way, detection of two Raman spectra with these slightly different excitation wavelengths leads to a small shift in the Raman band positions, while the broadband fluorescence background remains essentially unchanged. Subsequent subtraction of the spectra eliminates the fluorescence contribution and the detector fixed pattern

noise, whereas the characteristic Raman signals are preserved in the resulting derivative-like spectrum. A reconstruction by means of suitable algorithms, for example, using integration, produces a basically background-free SERDS spectrum revealing also weak Raman bands previously masked by fluorescence.

This has been demonstrated in the NIR spectral region by da Silva Martins et al. [8] applying a mechanically tunable laser in Littrow configuration for the investigation of human skin and tooth. However, to ensure highly reproducible and reliable operation, devices without moving parts would be preferable. Here, microsystem diode lasers with target-specific adjustable spectral properties according to the measurement task are well suited. Furthermore, their low power consumption as well as their compact size enables integration into portable systems suitable for SERDS application.

This paper presents SERDS investigations using microsystem diode lasers with two slightly shifted emission lines at 783 nm, 671 nm, and 488 nm as excitation light sources. The lasers emitting in the near-infrared and red spectral region were integrated into compact Raman measurement heads which are connected to laboratory (783 nm) as well as miniature spectrometers (671 nm), while the 488 nm light source is part of a laboratory setup. To test the performance of the SERDS technique, we chose meat, fat tissue, connective tissue, and bones from pork and beef as sample material to realize a variety of optical properties and fluorescence background levels.

2. Experimental

2.1. SERDS Setup for 783 nm Excitation. To realize a SERDS measurement head for near-infrared excitation, an in-house developed and tested Raman optical bench [9] was combined with a 783 nm distributed feedback (DFB) diode laser [10, 11]. By variation of the laser injection current from 110 mA to 260 mA, two operation points necessary to perform SERDS at $\lambda_1 = 782.65$ nm and $\lambda_2 = 783.15$ nm with a spectral shift of 0.5 nm (7 cm^{-1}) were realized. The laser temperature of 25°C as well as the injection current was controlled using a diode laser controller DC 100 (Toptica Photonics). Inside the Raman optical bench, the DFB diode laser beam is spectrally cleaned by a bandpass filter (AHF analysentechnik AG) and guided by dielectric mirrors and a Raman edge filter (Semrock, Inc.) to a lens with a focal length of 10 mm which focuses the excitation radiation through a quartz glass window onto the biological sample. All mirrors, lenses, as well as the quartz glass window were purchased from Thorlabs GmbH. The 180° backscattered radiation from the sample is collected by the above-mentioned focusing lens and passes a Raman edge filter to reject the Rayleigh as well as anti-Stokes components. Only the Raman Stokes scattering is transmitted and subsequently focused into an optical fiber with a core diameter of 100 μm by means of a lens with a focal length of 16 mm. A more detailed description of the concept of the Raman optical bench can be found in [12].

The SERDS measurement head is coupled to a PI 320 spectrometer (Princeton instruments) equipped with a 600 lines/mm grating. An attached back-illuminated deep-depletion CCD detector (DU4020-BR-DD, Andor Technology) thermoelectrically cooled down to −60°C serves for detection of the Raman spectra. CCD readout and data storage is performed by means of a computer running Andor Solis software (Andor Technology). With applied laser powers of 50 mW (782.65 nm) and 110 mW (783.15 nm) at sample position, Raman spectra of the biological samples were recorded with an integration time of 10 s.

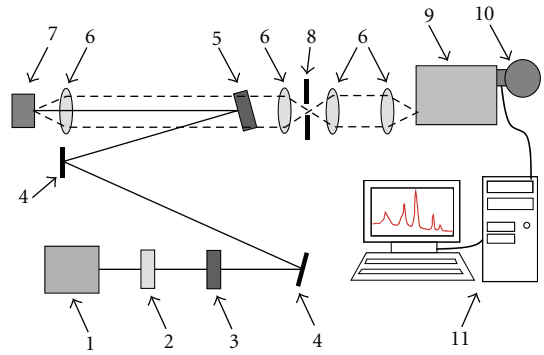

Figure 1: Scheme of experimental setup with (1) 488 nm microsystem diode laser, (2) BG 38 color glass filter, (3) bandpass filter, (4) dielectric mirror, (5) Raman edge filter, (6) lens, (7) sample, (8) pinhole, (9) spectrometer, (10) CCD, and (11) computer.

2.2. SERDS Setup for 671 nm Excitation. For the 671 nm measurement head, the same concept of a Raman optical bench with attached microsystem diode laser is applied. Here, the excitation light source contains two separate laser cavities each comprising a volume Bragg grating as frequency selective element [42]. Thus, two slightly different emission wavelengths at $\lambda_1 = 671.0$ nm and $\lambda_2 = 671.6$ nm with a spectral shift of 0.6 nm (12 cm^{-1}) are obtained. Two LDC 210C benchtop LD current controllers (Thorlabs GmbH) serve to control the injection current of 400 mA for both laser cavities, while the common heat sink temperature of 25°C was regulated by a DTC 100 temperature controller (Toptica Photonics). The SERDS measurement head is connected to a custom-designed miniature spectrometer (Horiba Scientific) with a resolution of 8 cm^{-1} by means of an optical fiber with a core diameter of 100 μm. A back-thinned CCD camera (S7031-1006, Hamamatsu) with 1024 × 58 pixel thermoelectrically cooled down to −10°C and a netbook running VersaSpec software (Horiba Scientific) were used to detect and record the Raman spectra. The integration time was set to 10 s, and the laser power at the sample amounts to 30 mW (671.0 nm) and 50 mW (671.6 nm).

2.3. SERDS Setup for 488 nm Excitation. The laboratory setup applied for Raman spectroscopic investigations at 488 nm is depicted in Figure 1. A 488 nm microsystem diode laser (1) based on second harmonic generation of a 976 nm DFB laser [43] serves as excitation light source. SERDS operation with a spectral shift of 0.3 nm (12 cm^{-1}) can be achieved by tuning of the laser temperature as well as of

the injection current which was controlled by a laser diode controller LDC 1000 (Profile Optische Systeme GmbH). In that way, an output at $\lambda_1 = 487.61$ nm is realized at an injection current of 350 mA and a temperature of 30°C, whereas emission at $\lambda_2 = 487.91$ nm is obtained with a current of 361 mA and a temperature of 38°C. Residual fundamental infrared radiation at 976 nm from the laser diode is removed by means of a BG 38 color glass filter (LOT Oriel group) (2). The 488 nm excitation radiation is spectrally cleaned using a bandpass filter (Semrock, Inc.) (3) and then transferred by dielectric mirrors (4) and a Raman edge filter (Semrock, Inc.) (5) to a lens (Thorlabs GmbH) (6) with a focal length of 30 mm. This lens focuses the laser beam through a quartz glass window (Linos GmbH) onto the sample (7) and also collects the backscattered radiation from the sample which then passes a Raman edge filter only transmitting the Stokes scattering while removing the Rayleigh as well as the anti-Stokes components. A subsequent spatial filter comprising two lenses (6) with focal lengths of 50 mm and 25 mm as well as a pinhole (8) with a diameter of 600 μm is applied to reject unwanted stray light. By means of a lens with a focal length of 50 mm, the Raman Stokes radiation is then focused onto an iHR320 spectrometer (Horiba Jobin Yvon) (9) and detected by a back-illuminated CCD detector (CCD-2048x512-BIUV-1LS) (10) cooled down to −130°C by liquid nitrogen. Applying a computer running Labspec software (Horiba Jobin Yvon) (11), Raman spectra of the meat component samples were recorded with laser powers of 20 mW (487.61 nm) and 26 mW (487.91 nm) at the sample position. The integration times amount to 4 s except for bone from beef which exhibits an extremely high fluorescence enabling an integration time of only 1 s.

2.4. Meat Components and Data Analysis. To obtain meat, fat, connective tissue, and bones from pork and beef, fresh meat slices including these components were bought in a local supermarket and investigated at the day of purchase. The biological tissue of interest was cut from the slices during sample preparation using a knife and transferred into Petri dishes to prevent it from drying. Until investigation, all sample material was stored in a laboratory refrigerator (Spezial-468, Philipp Kirsch, Germany) at 5°C. During the Raman measurement, each type of tissue was probed at 15 different positions and 10 spectra were averaged each. From the two slightly shifted Raman spectra of each measurement spot, SERDS spectra were calculated applying an in-house developed reconstruction procedure [44].

3. Results and Discussion

3.1. Meat from Pork and Beef. Figure 2 displays a comparative overview of Raman and SERDS spectra of meat from pork and beef applying excitation wavelengths of 783 nm, 671 nm, and 488 nm. As expected, the fluorescence level increases with decreasing excitation wavelength as can be seen at the different scales for the Raman intensity. Thus, for 783 nm excitation (Figure 2(a)), there is only a moderate fluorescence contribution. However, also here the advantage

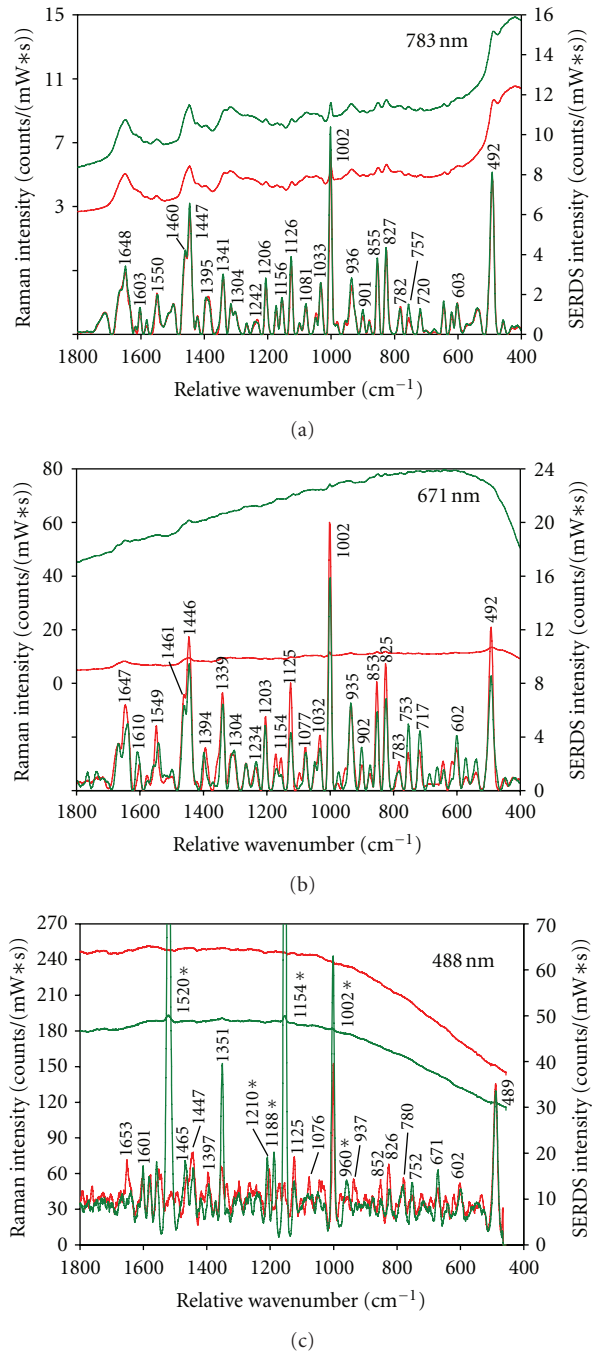

Figure 2: Comparison of Raman (upper traces) and SERDS spectra (lower traces) of meat from pork (red curves) and beef (green curves) excited at (a) 783 nm, (b) 671 nm, and (c) 488 nm. Each curve represents the average from 15 measurement positions. Resonance-enhanced carotenoid signals in (c) are indicated by asterisks.

of SERDS becomes obvious by effectively removing the background and leading to a straight horizontal baseline. In that way, normalization procedures on the net intensity of selected Raman bands often used for spectra comparison can be performed much easier. Numerous characteristic Raman signals of the meat protein structure can be identified

Table 1: Raman bands identified in the SERDS spectra of meat from beef and pork and their vibrational assignment, Phe: Phenylalanine, Trp: Tryptophan, Tyr: Tyrosine.

Vibrational assignment	783 nm excitation	671 nm excitation	488 nm excitation	Literature value [References]
Quartz	492	492	489	
Quartz	603	602	602	
Myoglobin	—	—	671	671–678 [13, 14]
Adenine	720	717	—	720 [15]
Trp	757	753	752	750–760 [16, 17]
Quartz	782	783	780	
Tyr ν-ring	827	825	826	827–834 [15, 16, 18]
Tyr ν-ring	855	853	852	850–860 [16]
Trp ν-ring	880	875	—	877–881 [15, 16]
νC–C	901	902	—	900–901 [16, 19]
νC–C	936	935	937	934–944 [16]
Carotenoid	—	—	960	960–965 [20]
Phe ν-ring	1002	1002	1001	1000–1006 [16, 17]
Carotenoid	—	—	1002	1000–1014 [21]
C–C ring bend (Phe)	1033	1032	—	1030–1033 [17, 19]
νC–N, νC–C	1047	1049	—	1040–1120 [19]
νC–N, νC–C	1081	1077	1076	1040–1120 [19]
νC–N	1126	1125	1125	1127–1130 [18, 22]
νC–C, δCOH	1156	1154	—	1156 [15]
Carotenoid	—	—	1154	1151–1172 [21]
Tyr	1173	1171	—	1172–1175 [15, 22]
Carotenoid	—	—	1188	1191–1193 [20]
Tyr, Phe	1206	1203	—	1205–1209 [17, 19]
Carotenoid	—	—	1210	1213–1215 [20]
Amide III (β-chain, random)	1242	1234	—	1225–1250 [19]
Amide III (α-helix)	1266	1266	—	1265–1278 [17, 19]
Amide III (α-helix)	1304	1304	—	1301–1309 [15, 16]
Trp; δCH	1341	1339	—	1339–1342 [15, 16, 19]
Myoglobin	—	—	1351	1353–1371 [13, 14]
δCH_3	1395	1394	1397	1395 [15]
$\delta_{as}CH_3$, δCH_2, δCH	1447	1446	1447	1447–1451 [17, 19]
CH_2 and CH_3 bending	1460	1461	1465	1460–1483 [16]
Carotenoid	—	—	1520	1511–1535 [21]
Trp ν-ring	1550	1549	—	1553-1554 [16]
Trp, Phe, Tyr ν-ring	1603	1610	1601	1605–1618 [15, 16]
Amide I (α-helix)	1648	1647	1653	1645–1658 [16, 18]

in the 783 nm SERDS spectra. Furthermore, weak signals as the tryptophan band at 757 cm^{-1} are clearly visible in the SERDS spectra and broad overlapping signals in the Raman spectra as the CH bending mode at 1341 cm^{-1} and the amide III band at 1304 cm^{-1} are resolved applying SERDS. An overview of the identified meat protein signals and their corresponding vibrational assignment according to the literature [15–19, 22] is presented in Table 1. The broad signal in the Raman spectra between 400 cm^{-1} and 500 cm^{-1} is due to the quartz window of the Raman measurement head. Here, it is remarkable that this quite broad band is reduced to a sharp peak around 490 cm^{-1} in the SERDS spectra which can be used for intensity normalization.

Applying an excitation wavelength of 671 nm results in a strongly increased fluorescence interference which becomes obvious in particular for beef as illustrated in Figure 2(b). However, the SERDS technique enables for an efficient background removal and all protein Raman bands which were present for 783 nm excitation can be identified also here. Furthermore, overlapping signals are resolved and weak bands can be clearly recognized.

Table 2: Raman bands identified in the SERDS spectra of fat tissue from beef and pork and their vibrational assignment.

Vibrational assignment	783 nm excitation	671 nm excitation	488 nm excitation	Literature value [References]
Quartz	492	494	490	
Quartz	605	606	607	
=C–H in-plane deformation	726	723	—	727 [23]
C–C stretch, CH_3 rock, C–O stretch	842	843	843	800–920 [24]
C–C stretch, CH_3 rock, C–O stretch	868	869	872	800–920 [24]
C–C stretch, CH_3 rock, C–O stretch	890	886	887	800–920 [24]
C–C stretch, CH_3 rock, C–O stretch	921	919	920	800–920 [24]
Carotenoid	—	—	960	960–965 [20]
=C–H out of plane bend *cis*	970	969	970	970–972 [23, 25, 26]
Carotenoid	—	—	1003	1000–1014 [21]
C–C aliphatic out-of-phase stretch	1061	1060	1060	1060–1068 [25, 26]
C–C aliphatic stretch	1084	1080	—	1076–1090 [23, 24, 26]
C–C aliphatic in phase stretch	1126	1125	1125	1119–1129 [23, 25]
Carotenoid	—	—	1153	1151–1172 [21]
Carotenoid	—	—	1188	1191–1193 [20]
Carotenoid	—	—	1211	1213–1215 [20]
=C–H symmetric rock *cis*	1262	1262	1263	1263–1266 [25, 27]
$>CH_2$ in phase twist	1297	1297	1294	1295–1305 [24, 26]
CH_3 symmetric deformation	1368	1368	1366	1368 [25]
$>CH_2$ symmetric deformation	1436	1436	1436	1436–1443 [25, 28, 29]
CH_3 antisymmetric deformation	1457	1459	1461	1455–1460 [25, 29]
Carotenoid	—	—	1521	1511–1535 [21]
C=C *cis* stretch	1651	1650	1653	1650–1670 [26]
Carbonyl C=O stretch	1740	1740	1738	1730–1750 [24]

Figure 2(c) displays the spectra from meat from pork and beef acquired with an excitation wavelength of 488 nm revealing an overwhelming fluorescence background masking all Raman signals except the major carotenoid bands in the case of beef. Nevertheless, SERDS allows for an efficient background removal and enables the identification of various Raman bands. In contrast to an excitation at 785 nm or 671 nm, the 488 nm SERDS spectra of beef contain characteristic carotenoid signals, marked by asterisks in Figure 2(c), which are enhanced by resonance Raman scattering. This comprises strong bands at 1002 cm^{-1}, 1154 cm^{-1}, and 1520 cm^{-1} [21] as well as minor signals at 960 cm^{-1}, 1188 cm^{-1}, and 1210 cm^{-1} [20]. In the pork meat spectra, these signals are completely absent enabling for a distinction between these two species. Furthermore, the tyrosine doublet at 826 cm^{-1} and 852 cm^{-1}, the 1002 cm^{-1} phenylalanine band (overlapping with a carotenoid signal for beef), and a CH bending vibration at 1447 cm^{-1} can be recognized in the SERDS spectra of beef and pork. The bands at 671 cm^{-1} and 1351 cm^{-1} which have higher signal intensities for beef than for pork might be attributed to myoglobin signals [13, 14], which are enhanced by the resonance Raman effect.

3.2. Fat from Pork and Beef. The recorded spectra for fat from pork and beef are presented in Figure 3. Excitation at 783 nm results in a moderate fluorescence interference, whereas the 671 nm spectra exhibit a significantly increased background for beef. However, application of SERDS leads to essentially background-free spectra in both cases clearly displaying all characteristic bands of fat tissue [23–29], which, are summarized in Table 2. Additionally, overlapping signals in the Raman spectra, for example, in the range between 800 cm^{-1} and 900 cm^{-1}, are clearly separated and resolved in the SERDS spectra.

Compared to meat, fat has a higher Raman scattering intensity and thus despite of the high fluorescence level even in the Raman spectra excited at 488 nm some strong lipid signals can be recognized (see Figure 3(c)). However, the SERDS technique allows for efficient background removal and reveals nearly all fat signals that were also present at excitation at 785 nm and 671 nm. Additionally, the carotenoid bands mentioned in Section 3.1 are present in fat from beef but absent in the pork samples. In that context, the improved resolution in the SERDS spectra can exemplarily be seen at the carotenoid signals located at 1153 cm^{-1}, 1188 cm^{-1}, and 1211 cm^{-1}, which are overlapping in the Raman spectra but are clearly separated using SERDS. In combination with the straight horizontal baseline this furthermore offers the potential to simplify quantitative carotenoid analysis in biological tissue.

3.3. Connective Tissue from Pork and Beef. Connective tissue possesses a complex Raman spectrum comprising a large number of collagen signals [30–34, 36] displayed in Figure 4

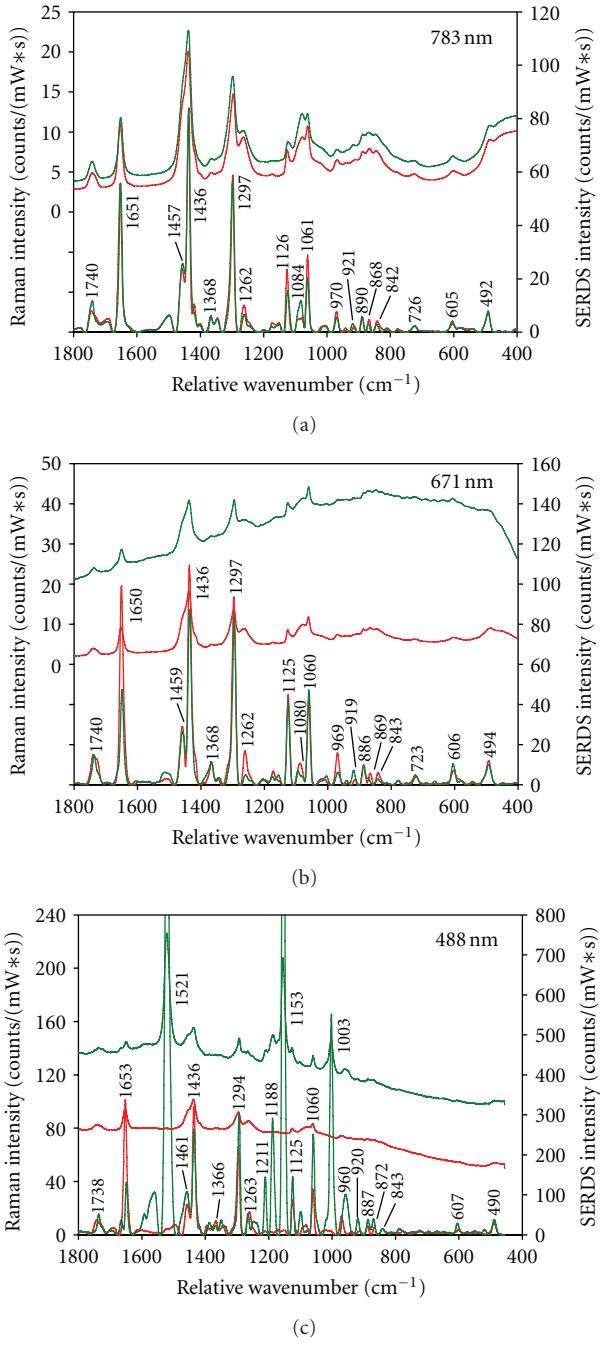

FIGURE 3: Comparison of Raman (upper traces) and SERDS spectra (lower traces) of fat from pork (red curves) and beef (green curves) excited at (a) 783 nm, (b) 671 nm, and (c) 488 nm. Each curve represents the average from 15 measurement positions.

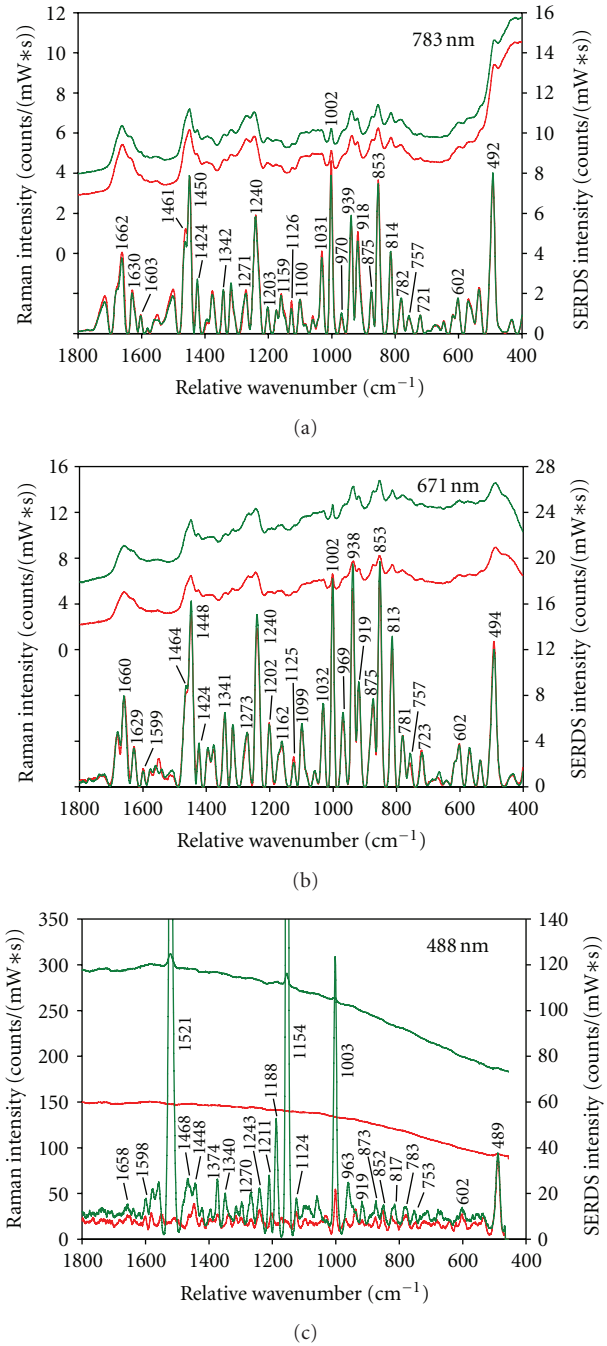

FIGURE 4: Comparison of Raman (upper traces) and SERDS spectra (lower traces) of connective tissue from pork (red curves) and beef (green curves) excited at (a) 783 nm, (b) 671 nm, and (c) 488 nm. Each curve represents the average from 15 measurement positions.

and summarized in Table 3. Here, the excitation wavelengths 783 nm and 671 nm cause only moderate fluorescence interference which allows revealing at least the major bands in the Raman spectra. Nevertheless, this type of biological sample is well suited to demonstrate the potential of SERDS because the Raman signature contains several weak and overlapping bands. In the essentially background-free SERDS spectra, this overlap issue is overcome since these signals are well separated and resolved as can be seen exemplarily in the ranges of 800–1000 cm^{-1} and 1200–1400 cm^{-1}. In that way, SERDS has a great potential for the investigation of complex biological samples with numerous and partly overlapping signals.

As in the case of meat, the Raman spectra of connective tissue excited at 488 nm presented in Figure 4(c) exhibit a

Table 3: Raman bands identified in the SERDS spectra of connective tissue from beef and pork and their vibrational assignment, Hyp: Hydroxyproline, Pro: Proline, Phe: Phenylalanine, Trp: Tryptophan, Tyr: Tyrosine.

Vibrational assignment	783 nm excitation	671 nm excitation	488 nm excitation	Literature value [References]
Quartz	492	494	489	
Quartz	602	602	602	
CH_2 rocking	721	723	—	730 [30]
Trp ring breathing	757	757	753	756 [30]
CH_2 rocking	782	781	783	779 [30]
ν(C–O–C); ν(C–C) of backbone	814	813	817	812–821 [31–33]
ν(C–C) of Pro ring	853	853	852	852–860 [32, 33]
ν(C–C) of Hyp ring	875	875	873	873–884 [31, 34]
ν(C–C) of Pro ring	918	919	919	920–925 [32, 33]
ν(C–C) of protein backbone	939	938	937	936–938 [32, 33]
Carotenoid	—	—	963	960–965 [20]
ν(C–C) of residue	970	969	—	957–961 [30, 31]
Phe	1002	1002	1002	1003–1006 [32, 33]
Carotenoid	—	—	1002	1000–1014 [21]
Phe, Pro	1031	1032	—	1032–1037 [31, 33]
Bend of carboxyl OH	1060	1058	—	1062–1065 [31]
ν(C–N)	1100	1099	—	1093–1101 [31, 35]
ν(C–N) of protein	1126	1125	1124	1122–1125 [36]
Carotenoid	—	—	1154	1151–1172 [21]
νCH_2, ρCH_3	1159	1162	—	1163 [30]
Carotenoid	—	—	1188	1191–1193 [20]
Hyp, Tyr	1203	1202	—	1202-1211 [33, 35]
Carotenoid	—	—	1211	1213–1215 [20]
Amide III	1240	1240	1243	1239–1248 [32, 33]
Amide III	1271	1273	1270	1263–1273 [30, 33]
CH_2 twisting	1318	1317	1314	1314–1319 [31, 33]
CH_2 wagging	1342	1341	1340	1340–1343 [31]
CH_2 deformation	1378	1377	1374	1379 [31]
$\nu_s(COO^-)$	1424	1424	1423	1416–1427 [32, 35]
$\delta(CH_3, CH_2)$	1450	1448	1448	1447–1452 [32, 33, 36]
$\delta(CH_3, CH_2)$	1461	1464	1468	1461–1464 [32, 33]
Carotenoid	—	—	1521	1511–1535 [21]
Phe, Tyr	1603	1599	1598	1603–1606 [32, 36]
Amide I	1630	1629	—	1636–1642 [32, 33]
Amide I	1662	1660	1658	1650–1680 [30]

very strong fluorescence influence making it impossible to determine any Raman signals except the resonance-enhanced carotenoid bands at 1003 cm^{-1}, 1154 cm^{-1}, and 1521 cm^{-1} for beef. The SERDS spectra allow for identification of various prominent collagen bands, for example, the 1002 cm^{-1} phenylalanine signal (overlapping with a carotenoid band for beef), the amide III band at 1243 cm^{-1} and 1270 cm^{-1} as well as CH_2 bending vibrations at 1374 cm^{-1} and 1448 cm^{-1}.

3.4. Bone from Pork and Beef. The Raman and SERDS spectra of bone from pork and beef are displayed in Figure 5. It is remarkable that even for excitation at 783 nm the bone from beef exhibits a significantly increased fluorescence background compared to meat, fat, and connective tissue. Here, the SERDS spectra allow for identification also of weak Raman bands like the phenylalanine signal at 1004 cm^{-1}. In addition, the SERDS technique demonstrates its ability to resolve overlapping signals exemplarily shown for the symmetric bending vibration of the phosphate group at 432 cm^{-1}. This band is overlapping with the broad quartz signal between 400 cm^{-1} and 500 cm^{-1} in the Raman spectra but can be clearly recognized in the SERDS spectra. The determined characteristic bone signals and their corresponding vibrational assignment using the literature [35, 37–41] are given in Table 4. However, several weak signals in the SERDS spectra were not mentioned in the previous works but could be attributed to the collagen matrix using the references mentioned in Section 3.3.

Table 4: Raman bands identified in the SERDS spectra of bone from beef and pork and their vibrational assignment, Hyp: Hydroxyproline, Pro: Proline, Phe: Phenylalanine, Tyr: Tyrosine.

Vibrational assignment	783 nm excitation	671 nm excitation	488 nm excitation	Literature value [References]
ν_2PO4^{3-}	432	432	—	422–454 [37]
$\nu_2PO_4^{3-}$	455	451	—	422–454 [37]
Quartz	494	494	489	
$\nu_4PO_4^{3-}$	583	583	581	578–617 [37]
ν_4PO4^{3-}	615	612	612	578–617 [37]
CH_2 rocking	723	719	—	730 [30]
CH_2 rocking	784	781	780	779 [30]
νC–C of collagen backbone	815	813	812	815 [38]
νC–C of Pro	853	851	850	855-856 [35]
νC–C of Hyp	880	884	—	871–876 [39]
νC–C of Pro	918	912	—	920-921 [35]
$\nu_1PO_4^{3-}$	958	958	957	957–963 [39]
Phe νCC ring	1004	1002	1001	1003-1004 [38, 40]
Carotenoid	—	—	1001	1000–1014 [21]
$\nu_3PO_4^{3-}$	1031	1030	1026	1030–1032 [39, 41]
$\nu_1CO_3^{2-}$,$\nu_3PO_4^{3-}$	1071	1070	1067	1065–1075 [37, 40]
ν(C–N)	1103	1099	1101	1093–1101 [31, 35]
ν(C–N) of protein	1128	1125	1125	1122–1125 [36]
Carotenoid	—	—	1155	1151–1172 [21]
νCH_2, ρCH_3	1161	1160	—	1163 [30]
Hyp, Tyr	1203	1200	1197	1202–1211 [33, 35]
Amide III	1243	1241	1241	1243–1320 [37]
Amide III	1272	1269	1266	1243–1320 [37]
Amide III	1320	1317	—	1243–1320 [37]
CH_2 wagging	1344	1341	1344	1340–1343 [31]
CH_2 deformation	1378	1375	1374	1379 [31]
δCH_2, scissoring	1450	1448	1447	1447–1452 [37]
$\delta(CH_3, CH_2)$	1464	1466	—	1461–1464 [32, 33]
Carotenoid	—	—	1518	1511–1535 [21]
Phe, Tyr	1603	1599	1602	1603–1606 [32, 36]
Amide I νC=O (α-helix)	1630	1629	1629	1640–1670 [38]
Amide I νC=O (α-helix)	1662	1658	1659	1640–1670 [38]
Amide I νC=O (α-helix)	1683	1681	1679	1640–1670 [38]

Using an excitation wavelength of 671 nm, the fluorescence interference is even more pronounced (see Figure 5(b)). However, the application of SERDS serves for an efficient background removal and enables obtaining essentially the same spectral pattern as for 783 nm excitation exhibiting all major and minor Raman signals.

The bone Raman and SERDS spectra excited at 488 nm are presented in Figure 5(c). Due to the overwhelming fluorescence background only the intense symmetric stretching vibration of the phosphate group at 957 cm^{-1} can be identified in the Raman spectra. Nevertheless, minor characteristic bone signals as the asymmetric bending (581 cm^{-1}) and stretching modes (1067 cm^{-1}) of the phosphate group are present in the SERDS spectra. Additionally, the amide III band at 1241 cm^{-1} as well as the CH_2 bending vibration at 1447 cm^{-1} of the collagen component in bone can be recognized. Resonance-enhanced carotenoid signals which were already found in meat, fat, and connective tissue from beef are also contained in bone from beef. However, only the major bands at 1001 cm^{-1}, 1155 cm^{-1}, and 1518 cm^{-1} are clearly visible.

4. Conclusion

In this paper, we applied shifted excitation Raman difference spectroscopy (SERDS) at different excitation wavelengths to demonstrate the potential for an efficient rejection of the fluorescence background in the Raman spectra of selected meat components. Microsystem diode lasers emitting at 783 nm, 671 nm, and 488 nm were used as excitation light sources. Each laser device was able to emit at two slightly different wavelengths with a spectral separation of about

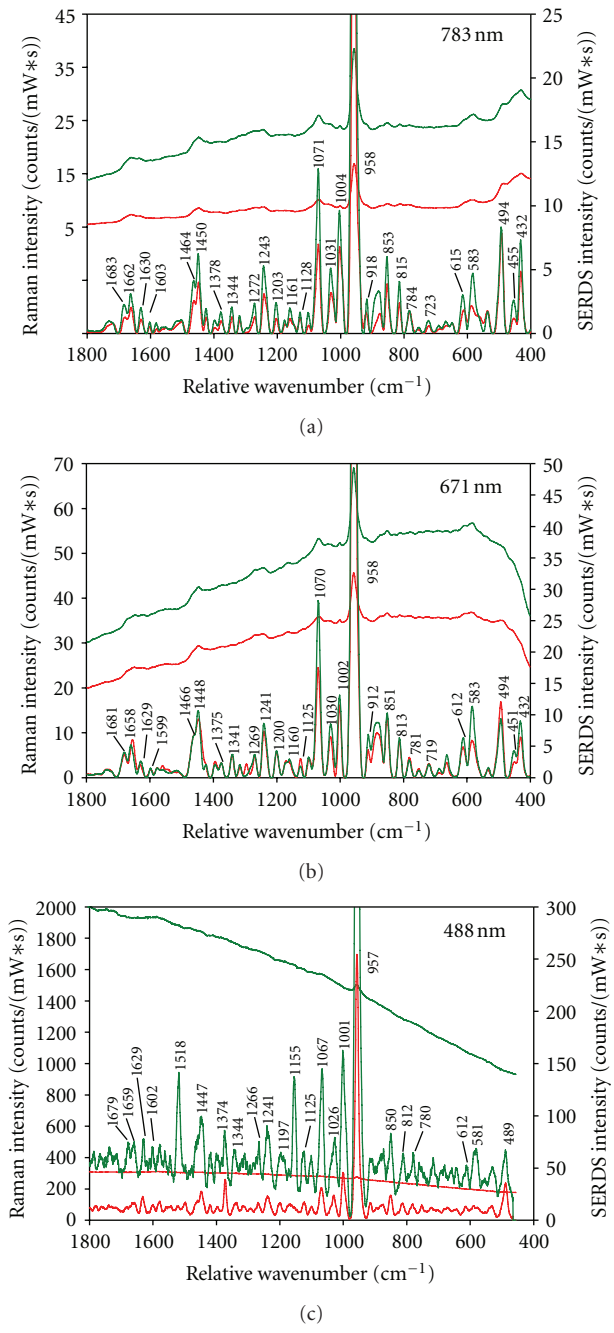

FIGURE 5: Comparison of Raman (upper traces) and SERDS spectra (lower traces) of bone from pork (red curves) and beef (green curves) excited at (a) 783 nm, (b) 671 nm, and (c) 488 nm. Each curve represents the average from 15 measurement positions.

$10\,\mathrm{cm}^{-1}$ necessary to perform SERDS. To realize a variety of biological samples, meat, fat, connective tissue, and bone from pork and beef were selected for our investigations.

With an excitation wavelength of 783 nm, the fluorescence interference was moderate. However, the SERDS technique effectively removed the signal background resulting in a straight horizontal baseline. Furthermore, weak bands in the Raman spectra become clearly visible in the SERDS spectra, and also overlapping signals are separated and resolved applying the SERDS technique.

An excitation at 671 nm results in an increased fluorescence background which becomes obvious in particular for the beef samples. Despite of this fluorescence issue, SERDS allows for efficient background removal enabling the identification of essentially the same spectral patterns of the samples under investigation as for 783 nm excitation.

As expected, the Raman spectra excited at 488 nm exhibit an overwhelming signal background masking nearly all Raman signals of the probed tissue except in the case of fat. Application of SERDS allows determining not all, but a majority of the signals which were present in the spectra excited at 783 nm and 671 nm. In addition, the tissue samples from beef reveal prominent signals of carotenoids which are enhanced by means of the resonance Raman effect. These bands are not present in samples from pork and thus allow for a rapid meat species distinction.

The presented study demonstrated the ability of the SERDS technique for an effective fluorescence background removal of selected biological material. Furthermore, weak bands are enhanced, and overlapping signals are resolved allowing for improvement of spectral quality. In that way, SERDS has a great potential for numerous other analytical Raman applications which were limited by the fluorescence issue up to now, for example, investigation of various natural compounds, medical diagnostics, and forensic usage.

Acknowledgments

The authors wish to thank Bernd Sumpf and Martin Maiwald, Ferdinand-Braun-Institut, Leibniz-Institut für Höchstfrequenztechnik Berlin, for the development of the microsystem diode laser sources suitable for SERDS emitting at 783 nm, 671 nm, and 488 nm. K. Sowoidnich is grateful for the financial support by the state of Berlin in the frame of an Elsa-Neumann scholarship.

References

[1] N. A. Marigheto, E. K. Kemsley, J. Potter, P. S. Belton, and R. H. Wilson, "Effects of sample heating in FT-Raman spectra of biological materials," *Spectrochimica Acta A*, vol. 52, no. 12, pp. 1571–1579, 1996.

[2] C. A. Lieber and A. Mahadevan-Jansen, "Automated method for subtraction of fluorescence from biological raman spectra," *Applied Spectroscopy*, vol. 57, no. 11, pp. 1363–1367, 2003.

[3] Z. M. Zhang, S. Chen, Y. Z. Liang et al., "An intelligent background-correction algorithm for highly fluorescent samples in Raman spectroscopy," *Journal of Raman Spectroscopy*, vol. 41, no. 6, pp. 659–669, 2010.

[4] N. Everall, T. Hahn, P. Matousek, A. W. Parker, and M. Towrie, "Picosecond time-resolved Raman spectroscopy of solids: capabilities and limitations for fluorescence rejection and the influence of diffuse reflectance," *Applied Spectroscopy*, vol. 55, no. 12, pp. 1701–1708, 2001.

[5] E. V. Efremov, J. B. Buijs, C. Gooijer, and F. Ariese, "Fluorescence rejection in resonance Raman spectroscopy using a picosecond-gated intensified charge-coupled device camera," *Applied Spectroscopy*, vol. 61, no. 6, pp. 571–578, 2007.

[6] A. P. Shreve, N. J. Cherepy, and R. A. Mathies, "Effective rejection of fluorescence interference in Raman spectroscopy using a shifted excitation difference technique," *Applied Spectroscopy*, vol. 46, no. 4, pp. 707–711, 1992.

[7] J. Zhao, M. M. Carrabba, and F. S. Allen, "Automated fluorescence rejection using shifted excitation Raman difference spectroscopy," *Applied Spectroscopy*, vol. 56, no. 7, pp. 834–845, 2002.

[8] M. A. da Silva Martins, D. G. Ribeiro, E. A. Pereira dos Santos, A. A. Martin, A. Fontes, and H. da Silva Martinho, "Shifted-excitation Raman difference spectroscopy for in vitro and in vivo biological samples analysis," *Biomedical Optics Express*, vol. 1, no. 2, pp. 617–626, 2010.

[9] H. Schmidt, K. Sowoidnich, M. Maiwald, B. Sumpf, and H. D. Kronfeldt, "Hand-held Raman sensor head for *in-situ* characterization of meat quality applying a microsystem 671 nm diode laser," in *Advanced Environmental, Chemical, and Biological Sensing Technologies VI*, vol. 7312 of *Proceedings of SPIE*, pp. 73120H-1–73120H-8, Orlando, Fla, USA, April 2009.

[10] H. Wenzel, A. Klehr, M. Braun et al., "High-power 783 nm distributed-feedback laser," *Electronics Letters*, vol. 40, no. 2, pp. 123–124, 2004.

[11] M. Maiwald, G. Erbert, A. Klehr et al., "Rapid shifted excitation Raman difference spectroscopy with a distributed feedback diode laser emitting at 785 nm," *Applied Physics B*, vol. 85, no. 4, pp. 509–512, 2006.

[12] H. Schmidt, K. Sowoidnich, and H. D. Kronfeldt, "A prototype hand-held raman sensor for the *in situ* characterization of meat quality," *Applied Spectroscopy*, vol. 64, no. 8, pp. 888–894, 2010.

[13] C. K. Johnson and R. Rubinovitz, "Near-infrared excitation of Raman scattering by chromophoric proteins," *Spectrochimica Acta A*, vol. 47, no. 9-10, pp. 1413–1421, 1991.

[14] V. Palaniappan and D. F. Bocian, "Acid-induced transformations of myoglobin. Characterization of a new equilibrium heme-pocket intermediate," *Biochemistry*, vol. 33, no. 47, pp. 14264–14274, 1994.

[15] U. Böcker, R. Ofstad, Z. Wu et al., "Revealing covariance structures in fourier transform infrared and Raman microspectroscopy spectra: a study on pork muscle fiber tissue subjected to different processing parameters," *Applied Spectroscopy*, vol. 61, no. 10, pp. 1032–1039, 2007.

[16] A. M. Herrero, "Raman spectroscopy for monitoring protein structure in muscle food systems," *Critical Reviews in Food Science and Nutrition*, vol. 48, no. 6, pp. 512–523, 2008.

[17] R. Tuma, "Raman spectroscopy of proteins: from peptides to large assemblies," *Journal of Raman Spectroscopy*, vol. 36, no. 4, pp. 307–319, 2005.

[18] M. Bouraoui, S. Nakai, and E. Li-Chan, "*In situ* investigation of protein structure in Pacific whiting surimi and gels using Raman spectroscopy," *Food Research International*, vol. 30, no. 1, pp. 65–72, 1997.

[19] E. B. Carew, I. M. Asher, and H. E. Stanley, "Laser Raman spectroscopy—new probe of myosin substructure," *Science*, vol. 188, no. 4191, pp. 933–936, 1975.

[20] S. P. Verma, J. R. Philippot, B. Bonnet, J. Sainte-Marie, Y. Moschetto, and D. F. H. Wallach, "Raman studies of structural rearrangements induced in human plasma lipoprotein carotenoids by malondialdehyde," *Lipids*, vol. 20, no. 12, pp. 890–896, 1985.

[21] V. E. de Oliveira, H. V. Castro, H. G. M. Edwards, and L. F. C. de Oliveiraa, "Carotenes and carotenoids in natural biological samples: a Raman spectroscopic analysis," *Journal of Raman Spectroscopy*, vol. 41, no. 6, pp. 642–650, 2010.

[22] M. Careche, A. M. Herrero, A. Rodriguez-Casado, M. L. Del Mazo, and P. Carmona, "Structural changes of hake (*Merluccius merluccius* L.) fillets: effects of freezing and frozen storage," *Journal of Agricultural and Food Chemistry*, vol. 47, no. 3, pp. 952–959, 1999.

[23] J. W. Chan, D. Motton, J. C. Rutledge, N. L. Keim, and T. Huser, "Raman spectroscopic analysis of biochemical changes in individual triglyceride-rich lipoproteins in the pre- and postprandial state," *Analytical Chemistry*, vol. 77, no. 18, pp. 5870–5876, 2005.

[24] J. R. Beattie, S. E. J. Bell, C. Borgaard, A. Fearon, and B. W. Moss, "Prediction of adipose tissue composition using Raman spectroscopy: average properties and individual fatty acids," *Lipids*, vol. 41, no. 3, pp. 287–294, 2006.

[25] L. B. Lyndgaard, K. M. Sørensen, F. van den Berg, and S. B. Engelsen, "Depth profiling of porcine adipose tissue by Raman spectroscopy," *Journal of Raman Spectroscopy*, vol. 43, no. 4, pp. 482–489, 2012.

[26] E. F. Olsen, C. Baustad, B. Egelandsdal, E.-O. Rukke, and T. Isaksson, "Long-term stability of a Raman instrument determining iodine value in pork adipose tissue," *Meat Science*, vol. 85, no. 1, pp. 1–6, 2010.

[27] E. F. Olsen, E.-O. Rukke, B. Egelandsdal, and T. Isaksson, "Determination of omega-6 and omega-3 fatty acids in pork adipose tissue with nondestructive raman and fourier transform infrared spectroscopy," *Applied Spectroscopy*, vol. 62, no. 9, pp. 968–974, 2008.

[28] E. F. Olsen, E.-O. Rukke, A. Flåtten, and T. Isaksson, "Quantitative determination of saturated-, monounsaturated- and polyunsaturated fatty acids in pork adipose tissue with nondestructive Raman spectroscopy," *Meat Science*, vol. 76, no. 4, pp. 628–634, 2007.

[29] S. P. Verma and D. F. H. Wallach, "Raman spectra of some saturated, unsaturated and deuterated c18 fatty acids in the HCH deformation and CH stretching regions," *Biochimica et Biophysica Acta*, vol. 486, no. 2, pp. 217–227, 1977.

[30] A. Tfayli, O. Piot, F. Draux, F. Pitre, and M. Manfait, "Molecular characterization of reconstructed skin model by Raman microspectroscopy: comparison with excised human skin," *Biopolymers*, vol. 87, no. 4, pp. 261–274, 2007.

[31] T. Ikoma, H. Kobayashi, J. Tanaka, D. Walsh, and S. Mann, "Physical properties of type I collagen extracted from fish scales of *Pagrus major* and *Oreochromis niloticas*," *International Journal of Biological Macromolecules*, vol. 32, no. 3–5, pp. 199–204, 2003.

[32] V. A. Iconomidou, M. E. Georgaka, G. D. Chryssikos, V. Gionis, P. Megalofonou, and S. J. Hamodrakas, "Dogfish egg case structural studies by ATR FT-IR and FT-Raman spectroscopy," *International Journal of Biological Macromolecules*, vol. 41, no. 1, pp. 102–108, 2007.

[33] B. G. Frushour and J. L. Koenig, "Raman scattering of collagen, gelatin, and elastin," *Biopolymers*, vol. 14, no. 2, pp. 379–391, 1975.

[34] H. G. M. Edwards, D. W. Farwell, J. M. Holder, and E. E. Lawson, "Fourier-transform Raman spectroscopy of ivory: II. Spectroscopic analysis and assignments," *Journal of Molecular Structure*, vol. 435, no. 1, pp. 49–58, 1997.

[35] J. Chen, C. Burger, C. V. Krishnan, B. Chu, B. S. Hsiao, and M. J. Glimcher, "In vitro mineralization of collagen in demineralized fish bone," *Macromolecular Chemistry and Physics*, vol. 206, no. 1, pp. 43–51, 2005.

[36] S. Jaisson, S. Lorimier, S. Ricard-Blum et al., "Impact of carbamylation on type I collagen conformational structure and

its ability to activate human polymorphonuclear neutrophils," *Chemistry and Biology*, vol. 13, no. 2, pp. 149–159, 2006.

[37] M. D. Morris and W. F. Finney, "Recent developments in Raman and infrared spectroscopy and imaging of bone tissue," *Spectroscopy*, vol. 18, no. 2, pp. 155–159, 2004.

[38] S. Le Blond, E. Guilminot, G. Lemoine, N. Huet, and J. Y. Mevellec, "FT-Raman spectroscopy: a positive means of evaluating the impact of whale bone preservation treatment," *Vibrational Spectroscopy*, vol. 51, no. 2, pp. 156–161, 2009.

[39] J. A. Timlin, A. Carden, M. D. Morris, R. M. Rajachar, and D. H. Kohn, "Raman spectroscopic imaging markers for fatigue-related microdamage in bovine bone," *Analytical Chemistry*, vol. 72, no. 10, pp. 2229–2236, 2000.

[40] G. McLaughlin and I. K. Lednev, "Spectroscopic discrimination of bone samples from various species," *American Journal of Analytical Chemistry*, vol. 3, no. 2, pp. 161–167, 2012.

[41] G. Penel, G. Leroy, C. Rey, and E. Bres, "MicroRaman spectral study of the PO_4 and CO_3 vibrational modes in synthetic and biological apatites," *Calcified Tissue International*, vol. 63, no. 6, pp. 475–481, 1998.

[42] M. Maiwald, H. Schmidt, B. Sumpf, G. Erbert, H. D. Kronfeldt, and G. Tränkle, "Microsystem 671nm light source for shifted excitation Raman difference spectroscopy," *Applied Optics*, vol. 48, no. 15, pp. 2789–2792, 2009.

[43] M. Maiwald, H. Schmidt, B. Sumpf et al., "Microsystem light source at 488 nm for shifted excitation resonance Raman difference spectroscopy," *Applied Spectroscopy*, vol. 63, no. 11, pp. 1283–1287, 2009.

[44] H. Schmidt, D. Pérez-Kaiser, and M. Maiwald, "Method for generating and for detecting a Raman spectrum," International Patent WO, 2011/033017 A1, 2011.